AIP | The Journal of Chemical Physics

Backbone NxH compounds at high pressures

Alexander F. Goncharov, Nicholas Holtgrewe, Guangrui Qian, Chaohao Hu, Artem R. Oganov, Maddury Somayazulu, Elissaios Stavrou, Chris J. Pickard, Adam Berlie, Fei Yen, Mahmood Mahmood, Sergey S. Lobanov, Zuzana Konôpková, and Vitali B. Prakapenka

Citation: The Journal of Chemical Physics **142**, 214308 (2015); doi: 10.1063/1.4922051
View online: http://dx.doi.org/10.1063/1.4922051
View Table of Contents: http://scitation.aip.org/content/aip/journal/jcp/142/21?ver=pdfcov
Published by the AIP Publishing

Backbone N_xH compounds at high pressures

Alexander F. Goncharov,[1,2,3] Nicholas Holtgrewe,[2,4] Guangrui Qian,[6,7,8] Chaohao Hu,[8] Artem R. Oganov,[5,6,7,8,9] Maddury Somayazulu,[2] Elissaios Stavrou,[2] Chris J. Pickard,[10] Adam Berlie,[1] Fei Yen,[1] Mahmood Mahmood,[4] Sergey S. Lobanov,[2,11] Zuzana Konôpková,[12] and Vitali B. Prakapenka[13]

[1]*Key Laboratory of Materials Physics, Institute of Solid State Physics, Chinese Academy of Sciences, 350 Shushanghu Road, Hefei, Anhui 230031, China*
[2]*Geophysical Laboratory, Carnegie Institution of Washington, 5251 Broad Branch Road, Washington, D.C. 20015, USA*
[3]*University of Science and Technology of China, Hefei, 230026, China*
[4]*Howard University, Washington, D.C. 20059, USA*
[5]*Skolkovo Institute of Science and Technology, Skolkovo Innovation Center, Moscow 143026, Russia*
[6]*Department of Geosciences, State University of New York, Stony Brook, New York 11794-2100, USA*
[7]*Center for Materials by Design, Institute for Advanced Computational Science, State University of New York, Stony Brook, New York 11794-2100, USA*
[8]*Guangxi Key Laboratory of Information Materials, Guilin University of Electronic Technology, Guilin 541004, China*
[9]*Moscow Institute of Physics and Technology, 9 Institutskiy Lane, Dolgoprudny, Moscow Region 141700, Russian Federation*
[10]*University College London, Gower St., London WC1E 6BT, United Kingdom*
[11]*V.S. Sobolev Institute of Geology and Mineralogy, SB RAS, 3 Pr. Ac. Koptyga, Novosibirsk 630090, Russia*
[12]*DESY Photon Science, Notkestrasse 85, D-22607 Hamburg, Germany*
[13]*Center for Advanced Radiation Sources, University of Chicago, Chicago, Illinois 60637, USA*

(Received 12 March 2015; accepted 22 May 2015; published online 5 June 2015)

Optical and synchrotron x-ray diffraction diamond anvil cell experiments have been combined with first-principles theoretical structure predictions to investigate mixtures of N_2 and H_2 up to 55 GPa. Our experiments show the formation of structurally complex van der Waals compounds [see also D. K. Spaulding *et al.*, Nat. Commun. **5**, 5739 (2014)] above 10 GPa. However, we found that these N_xH ($0.5 < x < 1.5$) compounds transform abruptly to new oligomeric materials through barochemistry above 47 GPa and photochemistry at pressures as low as 10 GPa. These oligomeric compounds can be recovered to ambient pressure at $T < 130$ K, whereas at room temperature, they can be metastable on pressure release down to 3.5 GPa. Extensive theoretical calculations show that such oligomeric materials become thermodynamically more stable in comparison to mixtures of N_2, H_2, and NH_3 above approximately 40 GPa. Our results suggest new pathways for synthesis of environmentally benign high energy-density materials. These materials could also exist as alternative planetary ices. © *2015 AIP Publishing LLC.* [http://dx.doi.org/10.1063/1.4922051]

I. INTRODUCTION

Chemistry of the N—H system is quite rich resulting in a number of known compounds that include ammonia, hydrazine, tetrazene, hydrazinium, and ammonium azides. However, only ammonia is a stable compound at ambient pressure, while others that have N—N bonds are metastable. Accordingly, planetary models assumed that ammonia would constitute a substantial amount of the interior of giant planets such as Uranus and Neptune.[1] On the other hand, metastable N—H compounds (as well as other nitrogen-rich systems) at ambient pressure would be superior high energy-density materials (HEDM) due to the substantial energy difference between single and triple nitrogen-nitrogen bonds (e.g., Ref. 2) (167 vs 942 kJ/mole, respectively). Additionally, such materials have much lower environmental and safety hazards compared to conventional energetic materials as their primary decomposition product is molecular nitrogen (N_2) and they have higher thermal stability. Although an exclusively nitrogenous material (e.g., cubic gauche nitrogen, cgN^3) would be the ultimate HEDM, retaining it at nearly-ambient conditions proved problematic. Moreover, synthesis of such materials requires very high pressures and temperatures, making it unpractical. Large polynitrogen molecules have been theoretically predicted but experimental realization has not been demonstrated.[4–6]

While synthesis of pure polymeric nitrogen at low pressures remains elusive, polymeric nitrogen-rich mixed materials would be a great alternative to commonly used explosives. There are numerous reports on synthesis of complex energetic materials containing chains of nitrogen atoms: N5, N8, and even N10[7–9] and complex "salts" such as TAG-MNT,[10] but these materials require other elements for stabilization and their synthesis remains quite challenging. Nitrogen-rich, long-chain N—H systems appear to be the most attractive as they would be having the highest energy-density. In general, the presence of hydrogen tends to stabilize nitrogen compounds with low bond order (e.g., hydrazine). In addition, the

thermodynamic and kinetic conditions, under which such long-chain molecules can be formed, are not well understood.

Application of high pressure provides an alternative to pure chemical routes for making new N—H materials as it stabilizes distinctive bonding schemes, such as single N—N bonds.[11] Indeed, recent theoretical work using *ab initio* evolutionary structure search predicted a new polymeric $(NH)_4$ hydronitrogen solid, which is more stable than ammonium azide and *trans*-tetrazene (TTZ) at pressures higher than 36 and 75 GPa, respectively.[12] However, using only thermodynamic stimuli is often insufficient to create new materials because of large kinetic barriers that could exist between different bonding configurations, which may require high temperature[3] or radiation[13–15] to initiate the reaction.

Previous experimental works on high-pressure behavior of N_2–H_2 mixtures found anomalous behavior of the N_2 and H_2 Raman vibron modes compared to pure materials.[16,17] Ciezak *et al.*[16] reported coexistence of two unidentified solid phases above 35 GPa, one of which was suggested to be amorphous based on a broadening of the Raman spectra and change in color. However, no definite conclusion about the chemical transformations could be made. Most recently, Spaulding *et al.*[18] independent to this study reported pressure-induced chemistry in a nitrogen-hydrogen host–guest structure. While their experimental results are similar to this work, they are interpreted differently.

In this work, we combined experiments and theory to address the questions raised about thermodynamic and kinetic stability of long-chain N—H compounds. We applied high pressure and irradiated the H_2–N_2 molecular mixtures to investigate the stability limits of this system in comparison with pure H_2 and N_2, which have been found to be stable to mbar pressures. We show that the N_2–H_2 system at pressures as low as 47 GPa is prone to molecular dissociation and formation of an oligomeric and/or polymeric N—H compound even at room temperature.[19] This unusual behavior is a unique example of mechanochemistry—the coupling of chemical processes and intermolecular interactions[20,21] (we will call it barochemistry here to avoid emphasizing anisotropic stresses which are characteristic of mechanochemistry); such phenomena have never been documented previously for simple diatomic molecules. Moreover, we find that application of a range of ultra-short pulses, from near ultraviolet (UV) (370 nm) to near infrared (IR) radiation (720 nm), causes a similar photochemical reaction even at 10 GPa. Our experimental observations are supported by the results of evolutionary and random structural searches, which show that oligomeric and/or polymeric N—H compounds of various stoichiometries become increasingly stable at high pressures. Our findings suggest that oligomeric/polymeric hydronitrogen compounds can be kinetically stable (i.e., metastable) at ambient pressure, while these materials become increasingly thermodynamically stable at high pressures suggesting that there can be planetary ices that could be distinct from the more commonly assumed ammonia.

II. MATERIALS AND METHODS

Molecular nitrogen and hydrogen were mixed in a high-pressure cylinder at 5-10 MPa. The sample composition was estimated based on the initial partial pressures. Based on this estimation, our samples of N_xH had composition x in the range of 0.5–1.5. Well homogenized molecular mixtures (homogenized over several days) were loaded in a symmetric diamond anvil cell at 200 MPa at room temperature. Then, the pressure was increased slowly and the samples were probed by *in situ* micro Raman and optical spectroscopy in visible and IR spectral ranges and synchrotron x-ray diffraction (XRD) (see below). The reaction products were unloaded at 297 and 80 K and the same techniques were used to monitor the recovered samples.

Raman studies were performed using 488 and 532 nm lines of a solid-state laser. The laser probing spot dimension was 4 μm. Raman spectra were analyzed with a spectral resolution of 4 cm^{-1} using a single-stage grating spectrograph equipped with a CCD array detector. Optical absorption spectra in the visible and IR spectral ranges were measured using an all-mirror custom microscope system coupled to a grating spectrometer equipped with a CCD detector.[22] X-ray diffraction measurements were performed at the undulator XRD beamline at GeoSoilEnviroCARS (GSECARS), APS, Chicago[23] and Extreme Conditions Beamline P02.2 at DESY (Germany). Typical X-ray beam size in all the experiments was 2-5 μm.

The high-pressure photochemistry was triggered by UV and visible radiation with ultra-short pulses (370, 580, and 720 nm) provided by an optical parametric amplifier (Coherent OPerA) with input pulses generated from a femtosecond oscillator combined with chirped pulse amplification (Coherent Mantis and Legend Elite). The radiation was focused in a spot of approximately 10 μm in diameter with an average power of 200 μW and the sample was irradiated for a few hours prior to analysis.

Predictions of stable phases were done using the USPEX code in the variable-composition mode.[24] The first generation of structures (up to 32 atoms per the primitive cell) was produced randomly and the succeeding generations were obtained by applying heredity, atom transmutation, and lattice mutation operations, with probabilities of 60%, 10%, and 30%, respectively. 80% non-identical structures of each generation with the lowest enthalpies were used to produce the next generation. All structures were relaxed using density functional theory (DFT) calculations within the Perdew-Burke-Ernzerhof (PBE),[25] as implemented in the VASP code.[26] Further *Ab Initio* Random Structures Searches (AIRSS)[27] were performed using the CASTEP code[28] with very similar results (the unit cells with up to 38 atoms were explored), and producing the structure which shows fair agreement with the experimental diffraction data.

III. RESULTS AND DISCUSSION

Raman spectroscopy, synchrotron XRD, and visual observations show that the mixture of molecular N_2 and H_2 remains a single-phase fluid up to 9-11 GPa and solidifies at higher pressure (Fig. 1(a)). The solid alloy forms crystallites (~10 μm) (Fig. 2); the Raman microprobe shows qualitatively similar spectra at various positions, which for some grains differ slightly in the Raman peak intensity, suggesting that

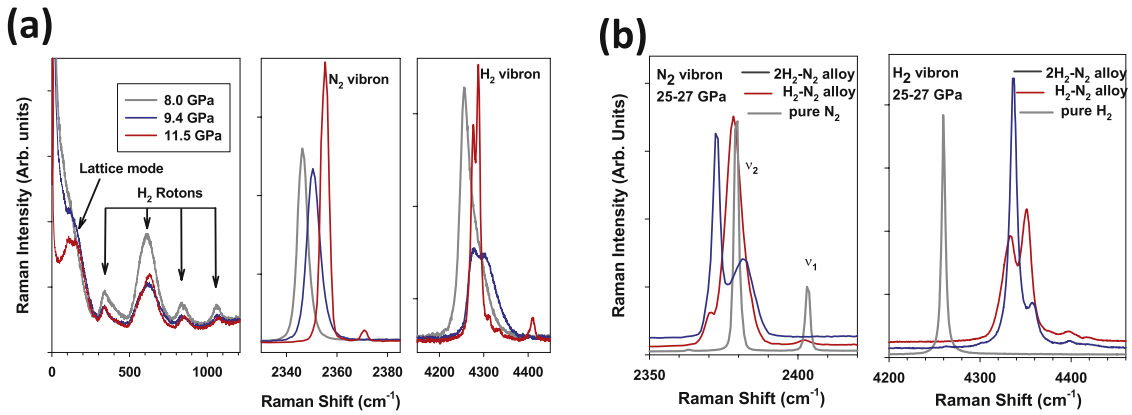

FIG. 1. Raman spectroscopy of the N_2–H_2 mixture. (a) Raman spectra through solidification. In a crystalline phase (at 11.5 GPa), a lattice mode develops near 150 cm^{-1} and there are minor changes in the H_2 rotational modes; also the vibron modes split and develop sidebands; (b) Raman vibron spectra of the N_2–H_2 mixture in comparison to those of pure N_2 and H_2 at 25-27 GPa. The Raman spectra of the N_2–H_2 compounds show a more complex vibron structure and broader peaks compared to the pure end-members.

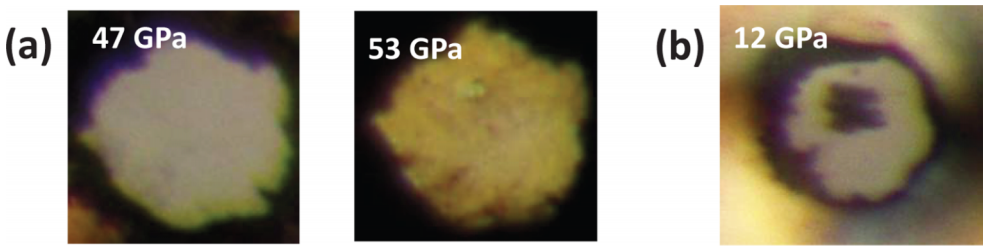

FIG. 2. Transformation of the H_2–N_2 van-der-Waals crystal at P > 47 GPa and 11.3 GPa: (a) microphotographs showing a change in color and grain structure; (b) image shows the formation of a new phase (a dark spot) after UV irradiation at 11.3 GPa.

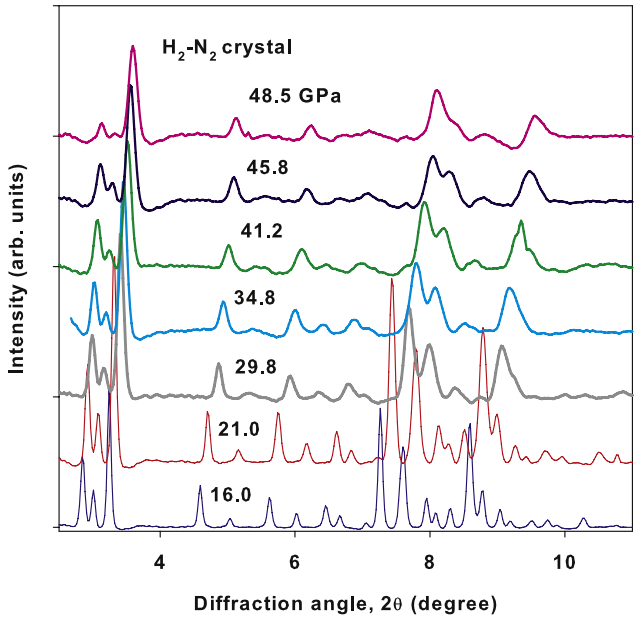

FIG. 3. X-ray diffraction patterns of a H_2–N_2 van-der-Waals compound as a function of pressure. The x-ray wavelength was 0.3344 Å.

the composition of crystallites can vary spatially. Given the complexity of the Raman spectra which cannot be described as a superposition of molecular N_2 and H_2 and the presence of the low-angle Bragg peaks in X-ray diffraction (see Figs. 1(b) and 3), this material can be characterized as a van-der-Waals (vdW) crystal with a large unit cell (see also Refs. 17 and 18); the crystal structure of this material will be reported elsewhere. Raman spectra of these materials show a variation of the vibron bands depending on composition (Fig. 1(b)), suggesting the existence of several different vdW compounds.

Above 47 GPa, substantial changes in the material vibrational and structural properties have been revealed by Raman, IR, and optical spectroscopy, as well as XRD (Figs. 4–6). The sample changes its appearance: it becomes yellowish as the optical bandgap develops in the visible near 2.5 eV and the micrograin structure changes (Figs. 2 and 5). Our Raman, optical, and X-ray microprobes show almost uniform properties of this material on a length scale of several micrometers (cf. Ref. 16). Above 47 GPa, Raman and IR observations showed time dependent responses with characteristic times of hours and even days (Figs. 4(a) and 4(b)). The most striking feature is a strong decrease in intensity of the vibron spectra of H_2 and N_2. The hydrogen vibron modes and the low-frequency rotational bands totally disappear suggesting a completion of the chemical reaction. A new system of broad bands appears at high pressures. One of these bands is slightly lower in frequency and much broader compared to the ν_2 N_2 vibron mode (Fig. 4(a)); the others have very different frequencies. Strong Raman and IR modes are observed near 3350, 1680, 1080, and 1300 cm^{-1} (Raman only) (Figs. 4(a) and 4(b)). Based on their frequencies, these bands can be tentatively assigned to the stretching and deformation (scissoring and rocking) N—H modes, and stretching N—N modes (see, for example, Ref. 29 for the mode assignment in hydrazine N_2H_2, which has a similar chemical structure), respectively. In addition, a broad

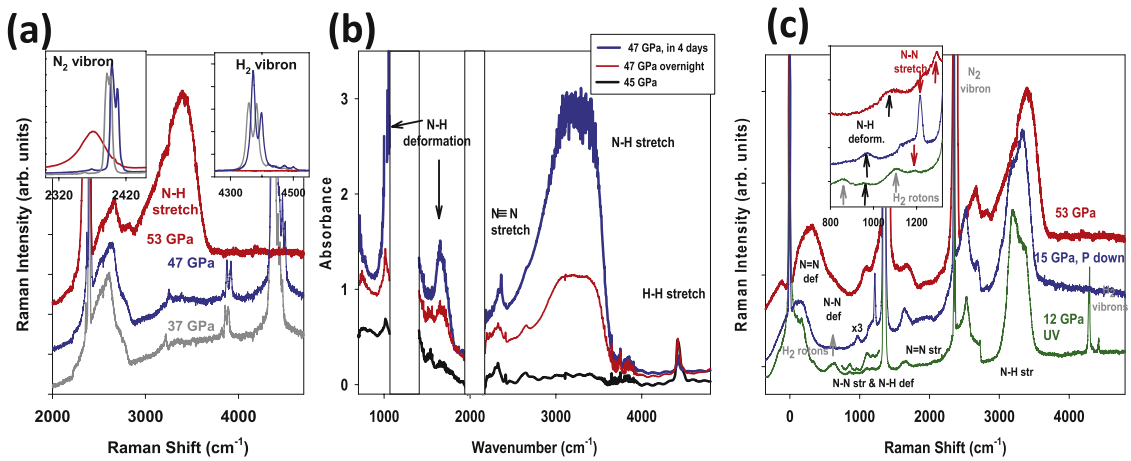

FIG. 4. Raman and IR spectroscopies of materials synthesized using baro- and photo-chemical reactions. In (a) and (b), the Raman and IR spectra evolution is shown to illustrate the reaction kinetics at 47-53 GPa. The Raman spectra at 53 GPa have been measured 4 days after measurements at 47 GPa; the pressure has only slightly increased during this time; time dependent changes have been observed at nominally constant pressure in Raman and IR experiments (b). The insets in (a) show details of the N_2 and H_2 vibron spectra. In (c), the two top curves correspond to the material synthesized above 47 GPa (red) and unloaded down to 15 GPa (blue); the bottom experimental curve (green)–to UV irradiated material. In (b), the spectral areas of large diamond anvil absorption are masked by boxes.

low-frequency strongly pressure dependent mode has been observed (Fig. 4(c)), which, based on this behavior, should be assigned to lattice translational/libration motions. X-ray diffraction patterns drastically change through the transition at 47 GPa, where narrow Bragg reflections of the mixed N_2–H_2 crystal phase disappear and are superseded by two systems of diffraction peaks: narrow and broad (Fig. 6).

Application of tightly focused pulsed radiation (370-720 nm, diameter ~4-6 μm) causes a similar transformation to occur at much lower pressure just after solidification (>10 GPa). Based on null observations from focusing continuous wave lasers (488 and 532 nm) and expanded femtosecond pulses (diameter ~20-30 μm) on the sample, this is thought to be a multi-photon process. We speculate this process involves avalanche photoionization followed by photoelectrons transfer energy into the lattice and finally energy induced chemical reaction[30] that involves disruption of N—N and H—H and formation of N—H bonds. Due to the high intensity of the electric field at the focal point (>10^{13} W/cm^2), many photons can be absorbed in the temporarily localized electron-ion plasma. The end result is the formation of various N—H bonds as shown by the N—H Raman modes in Fig. 4(c) (green curve). The complete transformation was difficult to establish even after a prolonged irradiation; thus, the new material coexists with unreacted sample in the high-pressure cavity (Fig. 4(c)). In contrast to the materials synthesized at high pressures (>47 GPa), that show a wide bandgap (Fig. 5), the irradiated material appears to be opaque and there are differences in relative intensities of the Raman bands (Fig. 4). Upon decompression at room temperature, the new phase stays intact down to 3.5 GPa, even though the surrounding unreacted material transitions back to liquid.

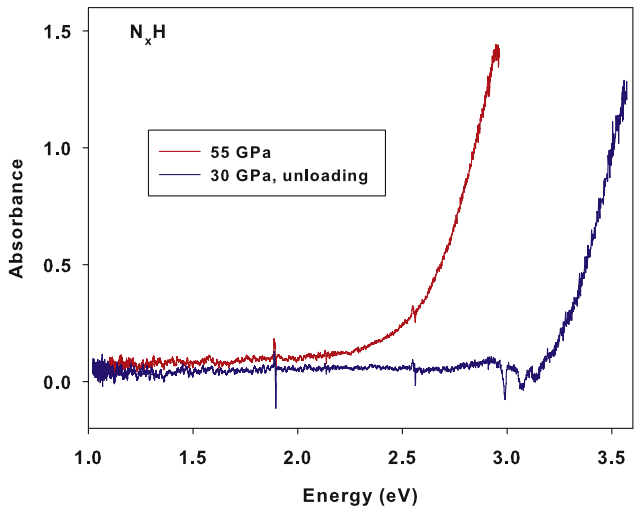

FIG. 5. Optical absorption spectra after the transformation to a high-pressure oligomeric phase at 55 GPa and at 30 GPa on the pressure decrease.

Vibrational spectroscopy data provide rather tight constraints on the chemical structure of the high-pressure phase we have synthesized. The absence of the H_2 roton and vibron modes clearly shows that the synthesized material does not have any H_2 molecules, free or weakly bounded. Given the vibrational frequencies observed, the data clearly indicate the formation of either oligomeric or polymeric single-bonded N—N chains (backbone) with the attached hydrogen atoms, as our Raman and IR spectra clearly reveal the formation of N—H (stretching and deformation) and N—N (single) bonds (Fig. 4). A more detailed comparison of experimentally observed IR and Raman frequencies with those calculated theoretically (see below) confirms this assignment. This interpretation explains all the observed Raman and IR modes (Fig. 4) and the absence of the H_2 roton and vibron modes with the exception of a broad, slightly red-shifted N_2 vibron mode described above (Fig. 4(a)). This broad band has been tentatively assigned to the presence of guest N_2 molecules embedded in the high-pressure phase matrix and/or nanosized (crystalline) nitrogen. A terminal triple bond vibration of N_8 complex predicted theoretically in Ref. 5 is expected at 2169 cm^{-1} (at 0 GPa), which is much lower than observed here (albeit at high pressures).

Additional information about the chemical structure of the synthesized products can be obtained based on the N—N

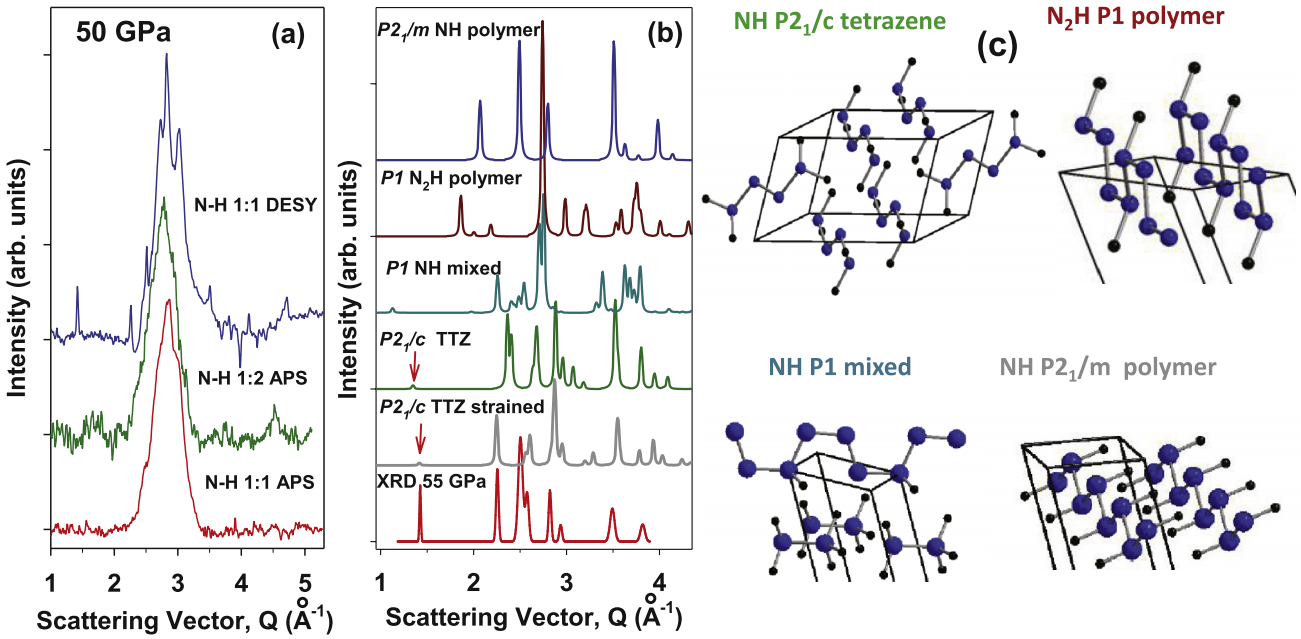

FIG. 6. X-ray diffraction of a high-pressure phase at 50-55 GPa. (a) A broad diffraction peak which supersedes narrow diffraction peaks at lower pressures (Fig. 3), the Compton background has been subtracted, the N:H composition is estimated based on the initial $N_2:H_2$ composition, barochemistry has been used in all experiments except for the 1:1 composition probed at GSECARS (the bottom curve): it was also irradiated at 10-12 GPa; (b) experimental diffraction pattern with narrow diffraction lines extracted from the 1:1 composition experiment at DESY in comparison to the computed patterns of the theoretically predicted N_xH structures at 50 GPa, this work and Ref. 12. Low-intensity low-angle Bragg peaks for the theoretically predicted TTZ $P2_1/c$ structures are marked by small vertical arrows. The patterns are plotted as a function of the scattering vector $Q = 4\pi\sin(\theta)/\lambda$, where 2θ is the diffraction angle, and λ is the X-ray wavelength (0.2893 Å at DESY and 0.3344 Å at APS); (c) the projections of the computed structures illustrating the presence of molecules and/or indefinitely long N—N chains.

stretch vibrational frequency(Fig. 7(a)). We used the high pressure behavior of hydrazine (H_2N–NH_2), which has similar vibrational spectra, as a reference. We find that the N—N stretch mode frequency of the material synthesized at high pressure is somewhat higher than that of hydrazine, while the same mode of the UV irradiated product is very close in frequency to hydrazine (Fig. 7(a)). Based on analogy with the better studied C—H system, where the C—C stretch frequency depends on the length of the —C—C— chain,[31] we suggest that the material synthesized at high pressure is oligomeric or polymeric (at least tetrameric), while that synthesized using UV irradiation consists of shorter N—N chains. Moreover, we find that the material unloaded to ambient pressure at low temperatures (80 K) shows the reduced value of the N—N stretch mode frequency (Fig. 7(a)), which is consistent with shortening of N—N chains at lower pressures.

The Raman and IR bands of newly synthesized N—H materials are broadened compared to common molecular solids (e.g., hydrazine), which suggests either large pressure gradients or due to compositional or structural defects. The latter is consistent with the fact that the transformation has been accomplished at room temperature, and thus has been a subject

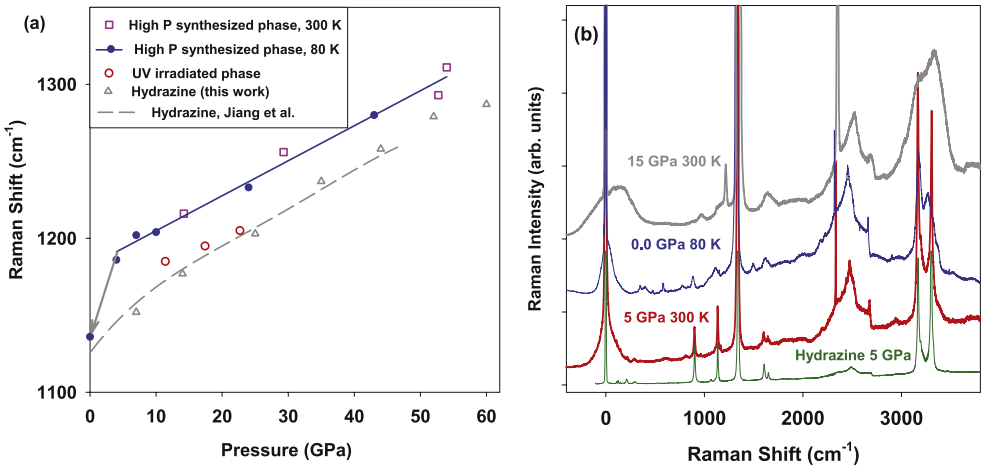

FIG. 7. Metastability of the synthesized at high pressure oligomeric material on the pressure decrease: (a) N—N stretching mode frequency; symbols: this work—different experiments; lines—guides to the eye; the arrow shows an abrupt change in frequency at unloading to 0 GPa at 80 K; the dashed line is the hydrazine data from Ref. 29. (b) Raman spectra: the bottom trace corresponds to hydrazine spectra at 5 GPa.

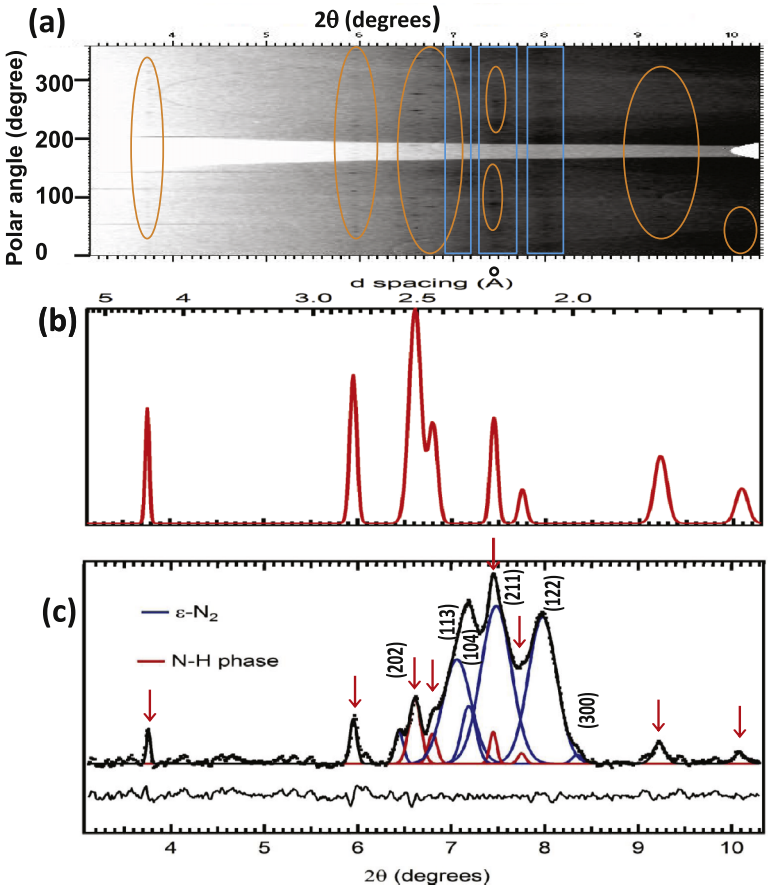

FIG. 8. X-ray diffraction pattern at 55 GPa after the transformation to the oligomeric phase. (a) 2D x-ray diffraction (cake), the ovals, and rectangles show the areas with diffraction of the new phase and molecular nitrogen, respectively; (b) extracted x-ray diffraction of a synthesized phase; (c) the deconvolution of peaks of molecular nitrogen (the main peaks are indexed) and oligomeric phase (marked by red arrows) in the integrated pattern. The x-ray wavelength was 0.2893 Å.

of kinetic and or steric hindrance (e.g., Ref. 32). We propose that this could result in the stacking defects as the formation of N—N long chains can be directionally frustrated. However, the presence of narrow diffraction lines in some experiments (Fig. 6) suggests that a long range order has been formed at least in some regions of the sample. Our attempts to anneal the stresses and inhomogeneities using gentle laser heating (<1000 K) caused the high-pressure phase to decompose; the obvious reaction product was molecular N_2.

The analysis of the diffraction patterns at 55 GPa (Figs. 6 and 8) shows that broadened XRD peaks correspond to ε-nitrogen[33] at somewhat lower pressure (45 GPa), the broadening being due to nanosized crystallites formed. This is in-line with the observation of broadened Raman N_2 vibron and a low-frequency lattice mode (Figs. 4(a) and 4(c)). The remaining (narrow) diffraction peaks were carefully chosen (Figs. 6 and 8); however, these data are not sufficient for performing an unequivocal indexing. The comparison of the experimental patterns with the theoretically predicted simulated ones reveals a qualitative agreement with the $P2_1/c$ TTZ. Apparent discrepancies, like the relative intensity of the low angle peaks (noted with the arrows in Figure 6), can be attributed to inherent experimental issues such as (a) errors related to subtraction of N_2 broad Bragg peaks which may affect final relative intensity, (b) strong texturing effects, and (c) possible difference in positional parameters between theory and experiment.

Further insight into possible crystal structure can be given based on theoretical calculations with the predictive power.[27,34] Polymeric structures in the N—H system become more stable at high pressures (e.g., Ref. 11). Search for the most stable structures with a variable N—H composition using evolutionary and random algorithms (USPEX[35] and AIRSS[27] codes) yielded a variety of different compositions and structures, the majority of which are quite complex and contain a large number of atoms. The detailed report of the study performed using USPEX will be published elsewhere.[36]

The detailed examination of the theoretically proposed N_xH structures and their enthalpies show that above 40 GPa, in addition to ammonia NH_3; the compounds with compositions NH and NH_2 become thermodynamically stable (Fig. 9). Two N_2H structures that are very close in enthalpy ($P1$ and $P2_1/c$) consist of N_4H_2 buckled infinite chains (Fig. 6). There are two very close in enthalpy structures for NH compounds: ($P1$ and $P2_1/c$) (Figs. 6, 9, and 10). Below 55 GPa, the stable one is $P2_1/c$, the structure (Fig. 6), which is similar to TTZ H_2N–N–N–NH_2 predicted in Ref. 12. The structure of the second one (called mixed) is more complex: it consists of interchanging layers of N_4H buckled infinite polymeric chains and N_2H_5 quasi-molecules (Fig. 6). The comparison of the experimental and theoretically predicted XRD shows a similarity for $P2_1/c$ tetrazene structure (Fig. 6), but much less resemblance to other structures predicted here and the $P2_1/m$ structure of Ref. 12. Moreover, we find that a small strain of $P2_1/c$ tetrazene structure (within 3.5% in lattice parameters) would make the agreement better (Fig. 6).

A detailed comparison of the experimental and theoretical Raman and IR spectra (Fig. 11) also suggests that $P2_1/c$ tetrazene is the compound synthesized at high pressures. Based

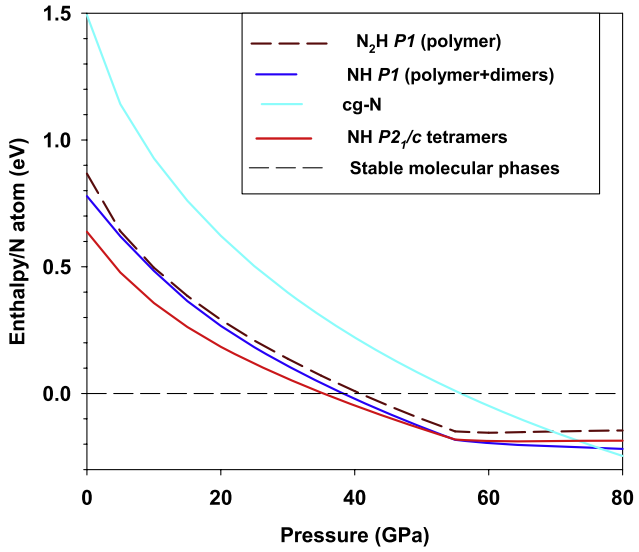

FIG. 9. The enthalpies of the most stable hydronitrogens and cg-N determined theoretically as a function of pressure (relative to a mixture of molecular phases).

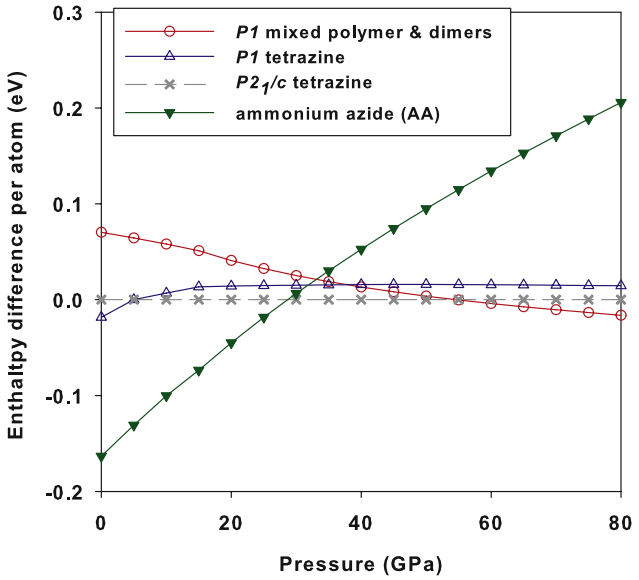

FIG. 10. The enthalpies of the most stable theoretically proposed in this work structures of hydronitrogens. The enthalpy of ammonium azide is shown for comparison. The transition to a tetrazene structure occurs near 27 GPa (cf. 36 GPa in Ref. 12).

on this comparison, we can safely rule out the N_2H polymeric compound and NH mixed polymer-dimer structure. However, taking into account a poor agreement of the diffraction data, we cannot completely rule out structures which are more complex or even slightly different from the predicted. Moreover, the material may be a mixture of several phases including those which we have predicted here. This is further supported by the proximity of the enthalpies (Figs. 9 and 10). However, we can safely rule out that the synthesized material is a simple mixture of hydronitrogens (known to form at ambient pressure), such as ammonia, hydrazine, and hydrazoic acid as these materials have different vibrational and structural properties at high pressure.[29,37]

We can further speculate that the structural disagreement (Fig. 6) may be attributed to the presence of defects due to frustration of the N—N bond directions in polymeric chains, thus resulting in various types of —N—N— oligomers to occur simultaneously. The presence of the N_2 inclusions or defects, which we have documented (Figs. 4(a), 4(c), and 8), can also affect the stress and structural state of hydronitrogens.

The high-pressure phase has a large range of (meta)stability as evident from Raman, IR absorption, and X-ray diffraction data which we obtained on pressure release (Fig. 7). At room temperature, the new phase is stable down to 15 GPa. At lower pressures, the material experiences decomposition, and the Raman and the IR spectra of the reaction products identify them as hydrazine (which we studied in a separate control high-pressure run, see also Ref. 29) and molecular nitrogen, N_2 (Fig. 7(b)). We have also performed a separate Raman experiment on unloading the high pressure phase at low temperatures (80 K), with the results showing its remarkable stability down to ambient pressure. The Raman bands (especially the N—H stretch modes) at low pressures and 80 K are substantially narrower than at high pressure/temperatures.

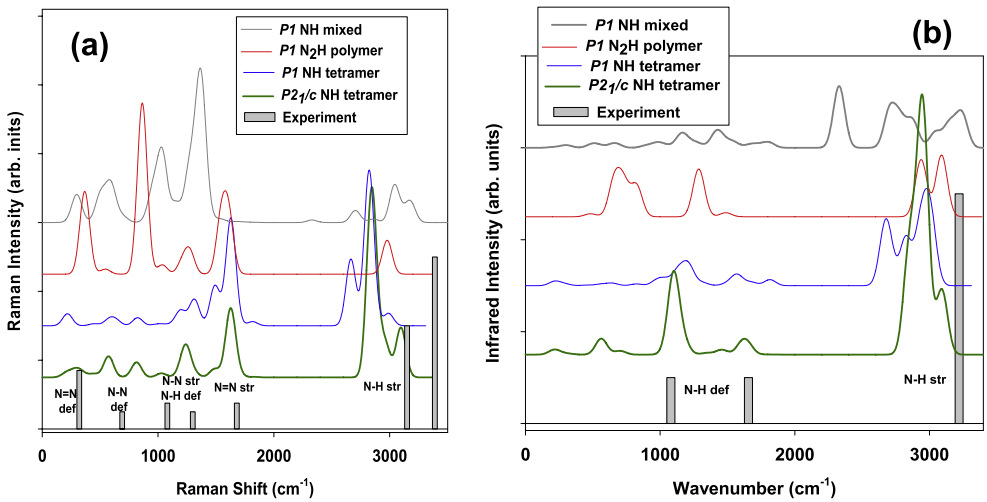

FIG. 11. Theoretically computed at 50 GPa Raman (a) and IR (b) spectra of the most stable hydronitrogens in comparison with the experimental data (at 55 GPa) for the compound synthesized at 47 GPa.

Moreover, some bands develop a structure with several components, but, nevertheless, the major spectral components remain supporting the conclusion about the metastability of the high-pressure phase (Fig. 7), although small traces of molecular N_2, H_2, and hydrazine are also observed. The Raman band, which is close in frequency to ν_2 N_2 vibron band as well a low-frequency lattice mode (Fig. 4(c)), rapidly drops in intensity at 0 GPa (80 K), indicating that these bands stem from interstitial and/or phase separated molecular N_2. The high-pressure phase rapidly decomposes (observed visually) forming again hydrazine (verified by Raman spectroscopy) on heating above 130 K.

It is remarkable that our experiment shows the transformation at pressures (47 GPa), which is only slightly higher than the predicted theoretically thermodynamic boundary (40 GPa, Fig. 9). The energy difference between the oligomeric and molecular states increases sharply below 40 GPa and it accounts approximately 60% of that of cgN at ambient pressure. The reverse transformation was found at about 15 GPa (300 K), suggesting that the experimental equilibrium transition pressure is near 31 GPa. Similarly, theory suggests that cgN is stable above 58 GPa (Fig. 4, see also Ref. 38), which is lower than the experimental pressure of 110 GPa.[2] We speculate that N_2 and H_2 molecules, forming a low-pressure inclusion compound (this work and Refs. 17 and 18), are kinetically prone for dissociation and formation of backbone NH chains even at room temperature. Here, we found that these molecules interact with each other in an unusual manner (see also Refs. 17 and 18), forming orientationally ordered inclusion compound that is clearly revealed in Raman vibron spectra (Fig. 1).

Exposure to intense radiation (primarily in the UV range) creates excited molecular states that reduce the kinetic barriers for chemical transformations because such excited states are less bounded, thus increasing the molecular polarizability and decreasing rotational barriers (e.g., Ref. 13). Assuming that the lowest-energy electronic excitations correspond to the Lyman-Birge-Hopfield band (see, e.g., Ref. 39) in the range of 9.3-10.2 eV (the ionization limit is near 16 eV)[40] and these molecular electronic excitations shift little with pressure below 10 GPa, we conjecture about the four-phonon absorption mechanism of our photoinduced reaction. This is consistent with extremely low efficiency of the process which we observed and its absence for when a slightly defocusing of the excitation beam was attempted to increase the reaction volume.

IV. CONCLUSIONS

Our combined experimental and theoretical studies of N_xH system provide a first unambiguous evidence of novel mechanochemistry and photochemistry which results in formation of oligomeric (or even polymeric) N—N backbone compounds some of which are recoverable to ambient pressure. First-principles DFT (Fig. 9) and simplistic bond energy calculations (Table I) show that materials synthesized here possess an energy yield up to 61% of that of cgN nitrogen depending on the length of the —N—N— chains. This finding enables search for technologically relevant synthesis techniques of such materials which holds a promise to be the choice for fuel of the future. While extreme pressures result in the synthesis of cgN and very moderate pressures result in the synthesis of NH_3 and hydrazine, we show that a combination of pressure, stress, varied composition, and photochemistry offers not only a plethora of hitherto unknown compounds but also a pathway to producing such HEDM materials that can be quenched to ambient pressure-temperature conditions. If stable at high temperature, the synthesized N—H compounds could be present as major components of planetary ices rather than the conventionally assumed ammonia ices. This seems plausible especially in view of the photolyzed reactivity, we observed at much lower pressures in this binary system.

TABLE I. Bond energies (kJ/mole) referred to N—N and H—H bond energies in diatomics.

Molecule	Structure	Reaction	$\Delta H_{reaction}$ (kJ/mol)[a,b]
N—H polymer[c]	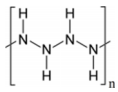	$(NH)_4 \rightarrow 2N_2 + 2H_2$	−134
Tetrazene		$(NH)_4 \rightarrow 2N_2 + 2H_2$	−113
Ammonium azide	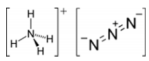	$(NH)_4 \rightarrow 2N_2 + 2H_2$	−92
Hydrazine		$2N_2H_4 \rightarrow 2N_2 + 4H_2$	−47.5
Ammonia		$4NH_3 \rightarrow 2N_2 + 6H_2$	+39
Cubic gauche nitrogen		$N_4 \rightarrow 2N_2$	−220.5

[a] All enthalpies of reaction are normalized to 1 nitrogen atom (e.g., Ammonium azide $\Delta H_{rxn} = -368$ kJ/mol for reaction with 4 nitrogen atoms on the reactants side. Normalized to 1 atom on reactants side equates to dividing the number of moles by 4 on both sides of the reaction, producing $\Delta H_{rxn} = -92$ kJ/mol).

[b] $\Delta H_{reaction}$ = [bonds broken] – [bonds formed]. Calculations are based on mean gas phase bond enthalpies only (values from taken from Engel and Reid, Ref. 41), enthalpy of sublimation (or vaporization) not taken into account.

[c] The synthesized material in this work is either a tetrazene or a mixed polymer-dimer.

ACKNOWLEDGMENTS

We thank Michael Armstrong for valuable comments and X.-J. Chen and Z. Zhi for supporting this work in China. We acknowledge support from the Army Research Office (No. W911NF-13-1-0231), DARPA (No. W31P4Q1210008), NSF (No. EAR-1128867), and NSFC (No. 21473211). X-ray diffraction experiments were performed at GeoSoilEnviro-CARS (Sector 13), Advanced Photon Source (APS), Argonne National Laboratory and Petra III, DESY, Hamburg, Germany. GeoSoilEnviroCARS is supported by the National Science Foundation—Earth Sciences (No. EAR-1128799) and Department of Energy—Geosciences (No. DE-FG02-94ER14466). Use of the Advanced Photon Source was supported by the U. S. Department of Energy, Office of Science, Office of Basic Energy Sciences, under Contract No. DE-AC02-06CH11357. PETRA III at DESY is a member of the Helmholtz Association (HGF). Theoretical calculations were supported by the National Science Foundation (Nos. EAR-1114313 and DMR-1231586), DARPA (Grant Nos. W31P4Q1210008 and W31P4Q1310005), the Government (No. 14.A12.31.0003) and the Ministry of Education and Science of Russian Federation (Project No. 8512) for financial support, and Foreign Talents Introduction and Academic Exchange Program (No. B08040). Calculations were performed on XSEDE facilities and on the cluster of the Center for Functional Nanomaterials, Brookhaven National Laboratory, which is supported by the DOE-BES under Contract No. DE-AC02-98CH10086. The research leading to these results has received funding from the European Community's Seventh Framework Programme (No. FP7/2007-2013) under grant Agreement No. 312284. C.H. acknowledges the support of the National Natural Science Foundation of China (Grants No. 11164005) and the Guangxi Natural Science Foundation (Grant No. 2014GXNSFGA118001). S.S.L. was partly supported by the Ministry of Education and Science of Russian Federation (Grant No. 14.B25.31.0032). M.S. acknowledges support from CDAC-NNSA.

[1]W. B. Hubbard, W. J. Nellis, A. C. Mitchell, N. C. Holmes, S. S. Limaye, and P. C. McCandless, Science **253**(5020), 648–651 (1991).
[2]M. Eremets, I. Trojan, A. Gavriliuk, and S. Medvedev, in *Static Compression of Energetic Materials*, edited by S. M. Peiris and G. J. Piermarini (Springer, Berlin, Heidelberg, 2008), pp. 75–97.
[3]M. I. Eremets, A. G. Gavriliuk, I. A. Trojan, D. A. Dzivenko, and R. Boehler, Nat. Mater. **3**(8), 558–563 (2004).
[4]P. C. Samartzis and A. M. Wodtke, Int. Rev. Phys. Chem. **25**(4), 527–552 (2006).
[5]B. Hirshberg, R. B. Gerber, and A. I. Krylov, Nat. Chem. **6**(1), 52–56 (2014).
[6]F. J. Owens, Comput. Theor. Chem. **966**(1–3), 137–139 (2011).
[7]K. O. Christe, W. W. Wilson, J. A. Sheehy, and J. A. Boatz, Angew. Chem., Int. Ed. **38**(13-14), 2004–2009 (1999).
[8]Y.-C. Li, C. Qi, S.-H. Li, H.-J. Zhang, C.-H. Sun, Y.-Z. Yu, and S.-P. Pang, J. Am. Chem. Soc. **132**(35), 12172–12173 (2010).
[9]T. M. Klapötke and D. G. Piercey, Inorg. Chem. **50**(7), 2732–2734 (2011).
[10]T. M. Klapötke, J. r. Stierstorfer, and A. U. Wallek, Chem. Mater. **20**(13), 4519–4530 (2008).
[11]V. V. Brazhkin and A. G. Lyapin, Nat. Mater. **3**(8), 497–500 (2004).
[12]A. Hu and F. Zhang, J. Phys.: Condens. Matter **23**, 022203 (2011).
[13]M. Ceppatelli, R. Bini, and V. Schettino, Proc. Natl. Acad. Sci. U. S. A. **106**(28), 11454–11459 (2009).
[14]W. L. Mao, H.-k. Mao, Y. Meng, P. J. Eng, M. Y. Hu, P. Chow, Y. Q. Cai, J. Shu, and R. J. Hemley, Science **314**(5799), 636–638 (2006).
[15]D. Chelazzi, M. Ceppatelli, M. Santoro, R. Bini, and V. Schettino, Nat. Mater. **3**(7), 470–475 (2004).
[16]J. A. Ciezak, T. A. Jenkins, and R. J. Hemley, AIP Conf. Proc. **1195**(1), 1291–1294 (2009).
[17]M. Kim and C.-S. Yoo, J. Chem. Phys. **134**(4), 044519 (2011).
[18]D. K. Spaulding, G. Weck, P. Loubeyre, F. Datchi, P. Dumas, and M. Hanfland, Nat. Commun. **5**, 5739 (2014).
[19]Here and below, we call oligomer a molecular complex that consists of a few N-H monomer units to distinguish it from polymer which forms much longer (at least 10 units) chains.
[20]J. J. Gilman, Science **274**(5284), 65 (1996).
[21]C. A. M. Seidel and R. Kuhnemuth, Nat. Nanotechnol. **9**(3), 164–165 (2014).
[22]A. F. Goncharov, P. Beck, V. V. Struzhkin, B. D. Haugen, and S. D. Jacobsen, Phys. Earth Planet. Inter. **174**(1-4), 24–32 (2009).
[23]V. B. Prakapenka, A. Kubo, A. Kuznetsov, A. Laskin, O. Shkurikhin, P. Dera, M. L. Rivers, and S. R. Sutton, High Pressure Res. **28**(3), 225–235 (2008).
[24]A. R. Oganov, Y. M. Ma, A. O. Lyakhov, M. Valle, and C. Gatti, Rev. Mineral. Geochem. **71**, 271–298 (2010).
[25]J. P. Perdew, K. Burke, and M. Ernzerhof, Phys. Rev. Lett. **77**(18), 3865–3868 (1996).
[26]G. Kresse and J. Furthmüller, Comput. Mater. Sci. **6**(1), 15–50 (1996).
[27]C. J. Pickard and R. J. Needs, J. Phys.: Condens. Matter **23**(5), 053201 (2011).
[28]S. J. Clark, M. D. Segall, C. J. Pickard, P. J. Hasnip, M. J. Probert, K. Refson, and M. C. Payne, Z. Kristallogr. **220**, 567–570 (2005).
[29]S. Jiang, X. Huang, D. Duan, S. Zheng, F. Li, X. Yang, Q. Zhou, B. Liu, and T. Cui, J. Phys. Chem. C **118**(6), 3236–3243 (2014).
[30]A. Royon, Y. Petit, G. Papon, M. Richardson, and L. Canioni, Opt. Mater. Express **1**(5), 866–882 (2011).
[31]T. Shimanouchi, Pure Appl. Chem. **36**, 93–108 (1973).
[32]V. Schettino and R. Bini, Phys. Chem. Chem. Phys. **5**(10), 1951–1965 (2003).
[33]E. Gregoryanz, A. F. Goncharov, C. Sanloup, M. Somayazulu, H.-k. Mao, and R. J. Hemley, J. Chem. Phys. **126**(18), 184505 (2007).
[34]A. R. Oganov and C. W. Glass, J. Chem. Phys. **124**(24), 244704 (2006).
[35]A. O. Lyakhov, A. R. Oganov, H. T. Stokes, and Q. Zhu, Comput. Phys. Commun. **184**(4), 1172–1182 (2013).
[36]G.-R. Qian, C.-H. Hu, A. R. Oganov, Q. Zeng, and H.-Y. Zhou; e-print arXiv:1411.4513 (2014).
[37]S. Ninet, F. Datchi, and A. M. Saitta, Phys. Rev. Lett. **108**(16), 165702 (2012).
[38]C. J. Pickard and R. J. Needs, Phys. Rev. Lett. **102**(12), 125702 (2009).
[39]D. J. McEwen and R. W. Nicholls, Nature **209**(5026), 902 (1966).
[40]J. A. Bradley, A. Sakko, G. T. Seidler, A. Rubio, M. Hakala, K. Hämäläinen, G. Cooper, A. P. Hitchcock, K. Schlimmer, and K. P. Nagle, Phys. Rev. A **84**(2), 022510 (2011).
[41]T. Engel and P. J. Reid, *Physical Chemistry*, 3rd ed. (Prentice Hall, 2012).